Electronic Supplementary Material (ESI) for Integrative Biology.

Supplemental Information

Interstitial fluid pressure regulates collective invasion in engineered human breast tumors via Snail, vimentin, and E-cadherin

Alexandra S. Piotrowski-Daspit, Joe Tien, and Celeste M. Nelson

Supplementary Tables and Figures

Table S1. Primers used for quantitative real-time reverse-transcription PCR (RT-PCR)

gene	sequences
18S rRNA	Fwd: CGGCGACGACCCATTCGAAC Rev: GAATCGAACCCTGATTCCCCGTC
VIM	Fwd: ATCAACACCGAGTTCAAG Rev: GCCAGCAGGATCTTATTC
SNAI1	Fwd: CCACTCAGATGTCAAGAAG Rev: GCAGGTATGGAGAGGAAG
CDH1	Fwd: CTAATTCTGATTCTGCTGCTCTTG Rev: CCTCTTCTCCGCCTCCTTC
KRT8	Fwd: AGTTACGGTCAACCAGAG Rev: GTCTCCAGCATCTTGTTC

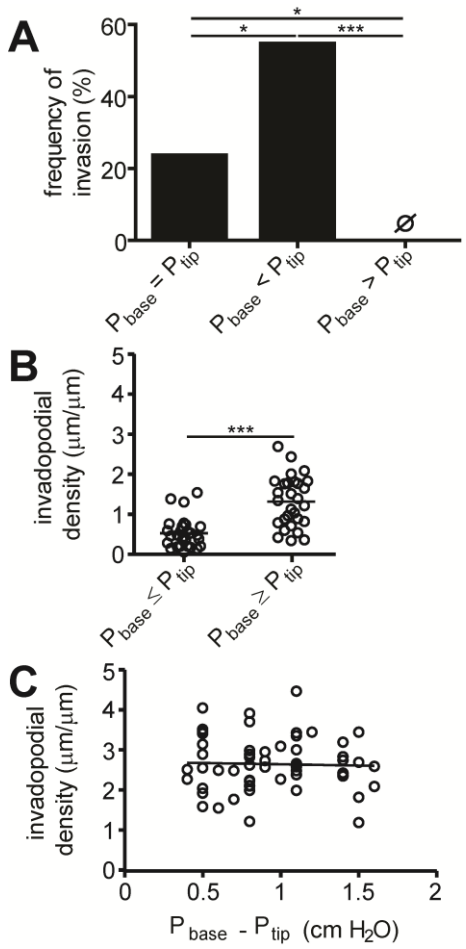

Figure S1. IFP controls invasive phenotype of breast and prostate cancer cells. (**A**) Frequency of invasion of PC-3 cell aggregates under $P_{base}=P_{tip}$ (n = 27), $P_{base}<P_{tip}$ (n = 20), or $P_{base}>P_{tip}$ (n = 17). (**B**) Invadopodial length density for MDA-MB-231 cell aggregates under $P_{base}\leq P_{tip}$ or $P_{base}\geq P_{tip}$. (**C**) Invadopodial density as a function of pressure profile for MDA-MB-231 breast cancer aggregates. The solid line denotes the best least-squares linear fit. * P<0.05, ** P<0.01, *** P<0.001.

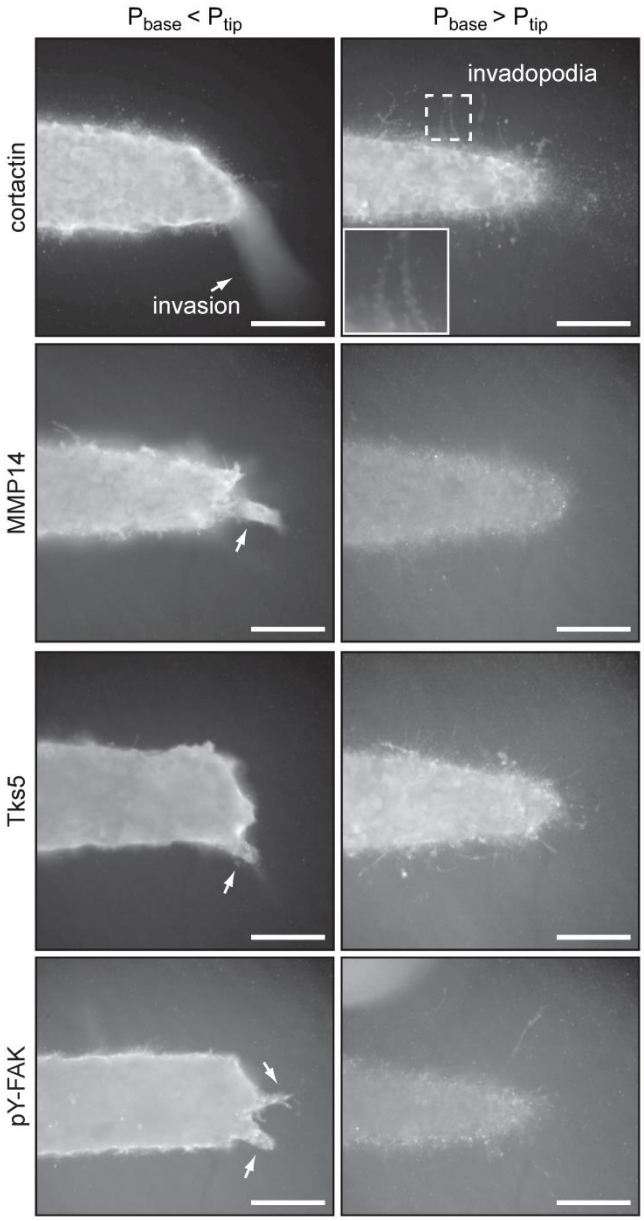

Figure S2. Confocal images of immunofluorescence stains for cortactin, MMP14, Tks5, and phosphorylated FAK (pY-FAK) in MDA-MB-231 cell aggregates under IFP. Arrows denote invasive protrusions containing multiple nuclei; the inset in the right cortactin image magnifies the dotted area. Scale bars, 100 μm.

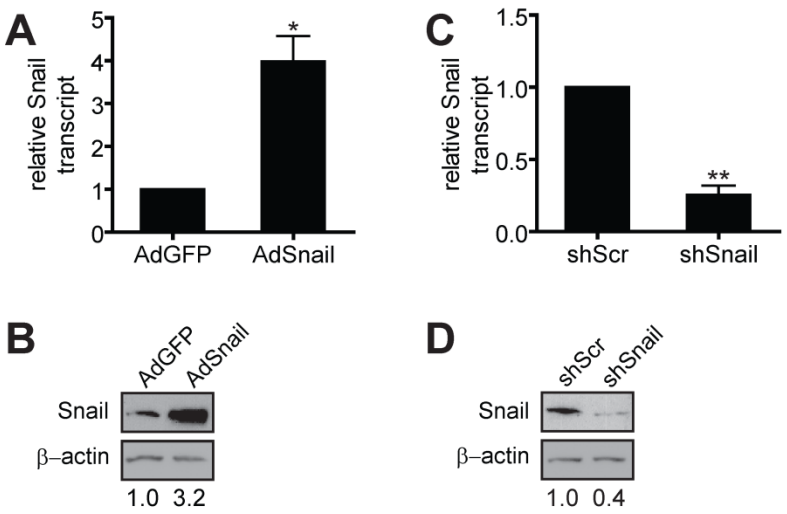

Figure S3. Snail expression in MDA-MB-231 cells. (**A**) Relative transcript levels of Snail in AdSnail (n = 3) or AdGFP (n = 4) MDA-MB-231 cells. (**B**) Immunoblot analysis of MDA-MB-231 cells transduced with AdGFP or AdSnail. (**C**) Relative transcript levels of Snail in shScr (n = 3) or shSnail (n = 3) MDA-MB-231 cells. (**D**) Immunoblot analysis for Snail in shScr and shSnail MDA-MB-231 cells. * P<0.05, ** P<0.01.

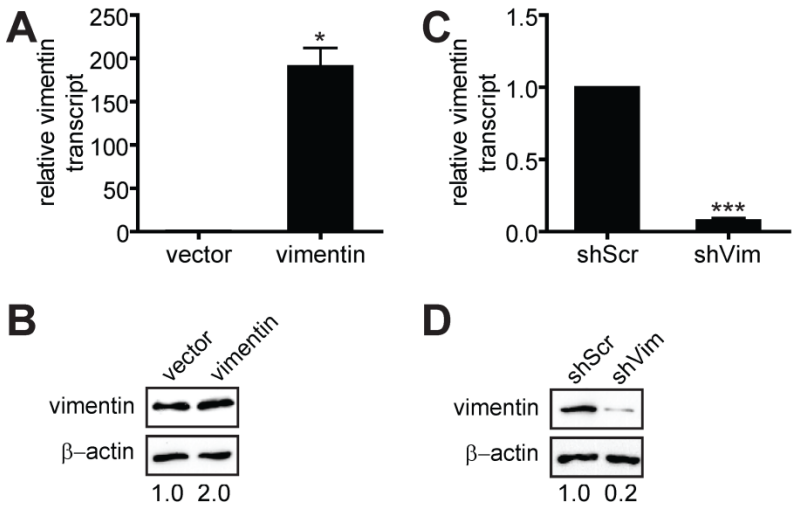

Figure S4. Vimentin expression in MDA-MB-231 cells. (**A**) Relative transcript levels of vimentin in vector (n = 3) or vimentin (n = 3) MDA-MB-231 cells. (**B**) Immunoblot of vector or vimentin MDA-MB-231 cells. (**C**) Relative transcript levels of vimentin in shScr (n = 3) or shVim (n = 3) MDA-MB-231 cells. (**D**) Immunoblot analysis for vimentin in shScr or shVim MDA-MB-231 cells. * P<0.05, *** P<0.001.

Figure S5.

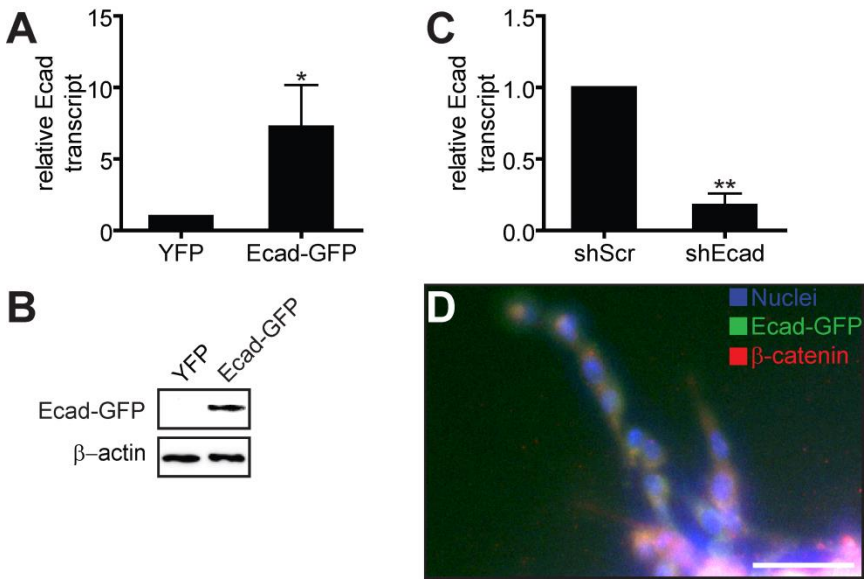

Figure S5. E-cadherin expression in MDA-MB-231 cells. (**A**) Relative transcript levels of E-cadherin in YFP (n = 3) or Ecad-GFP (n = 3) MDA-MB-231 cells. (**B**) Immunoblot analysis for E-cadherin in YFP or Ecad-GFP MDA-MB-231 cells. (**C**) Relative transcript levels of E-cadherin in shScr (n = 3) or shEcad (n = 3) MDA-MB-231 cells. (**D**) Immunofluorescence staining for β-catenin (red) and Hoechst 33342 staining of cell nuclei (blue) in invasions from an Ecad-GFP (green) aggregate under $P_{base}<P_{tip}$. * $P<0.05$, ** $P<0.01$. Scale bar, 25 μm.

Figure S6.

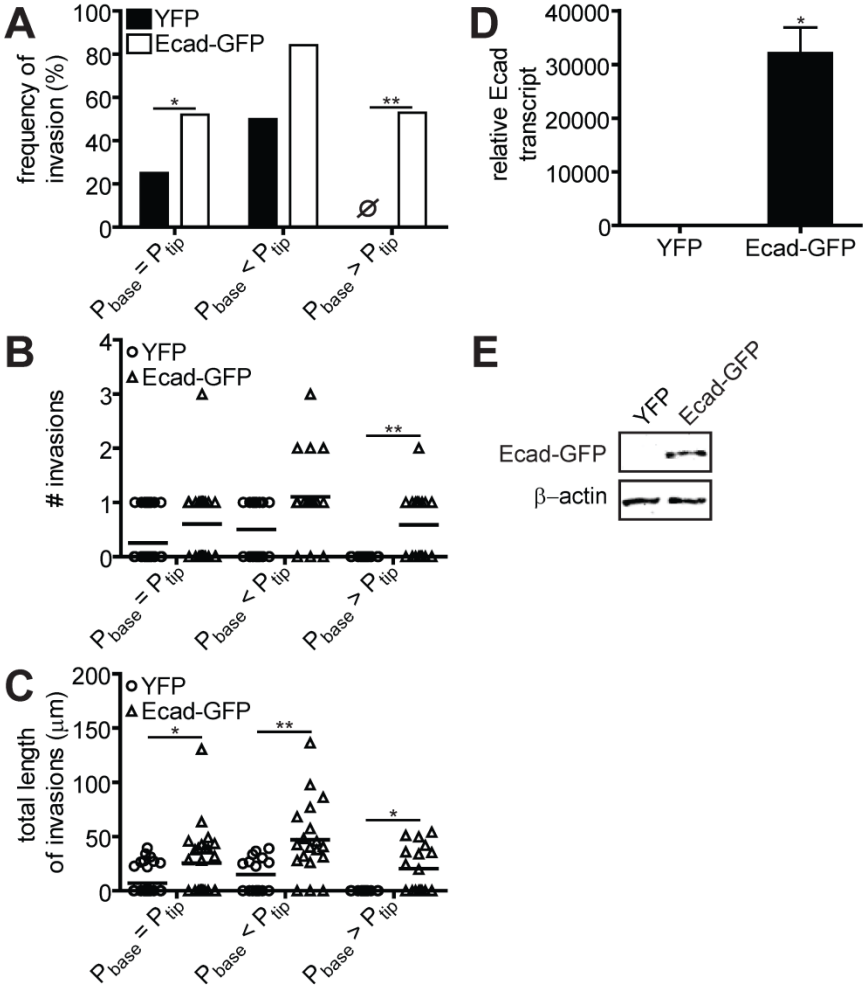

Figure S6. Ectopic expression of E-cadherin promotes invasion, whereas depletion of E-cadherin inhibits extensive invasion in response to IFP in PC-3 cells. (**A**) Frequency of invasion of YFP or Ecad-GFP-expressing PC-3 aggregates under $P_{base}=P_{tip}$ (YFP: n = 36; Ecad-GFP: n = 25), $P_{base}<P_{tip}$ (YFP: n = 16; Ecad-GFP: n = 19), or $P_{base}>P_{tip}$ (YFP: n = 15; Ecad-GFP: n = 17). (**B**) Number and (**C**) length of invasions in YFP or Ecad-GFP PC-3 aggregates under IFP. (**D**) Relative transcript levels of E-cadherin in YFP (n = 3) or Ecad-GFP (n = 3) PC-3 cells. (**E**) Immunoblot analysis for E-cadherin in YFP- or Ecad-GFP-transfected PC-3 cells. * P<0.05, ** P<0.01.